

Influence of compaction procedure on the mechanical behaviour of an unsaturated compacted clay. Part 2: shearing and constitutive modelling

S. J. WHEELER* and V. SIVAKUMAR†

The influence of compaction pressure, compaction water content and type of compaction (static or dynamic) on subsequent soil behaviour was investigated by conducting controlled-suction triaxial tests on samples of unsaturated compacted speswhite kaolin. Compaction pressure influences initial state, by determining the initial position of the yield surface, thus affecting, among other things, the shape of stress–strain curves during shearing. Compaction pressure also influences, to a limited degree, the positions of the normal compression lines for different values of suction, but it has no effect on critical state relationships. The effect of compaction pressure can probably be modelled solely in terms of initial state if an anisotropic elastoplastic model incorporating rotational hardening is employed, whereas the parameters defining the slopes and intercepts of the normal compression lines for different values of suction require adjustment with variation of compaction pressure if a conventional isotropic hardening elastoplastic model is employed. Compaction water content influences the initial suction, but also has a substantial influence on normal compression lines and a noticeable effect on the volumetric behaviour at critical states. It is likely that soil samples compacted at different water contents will have to be modelled as different materials, irrespective of whether an isotropic or anisotropic hardening elastoplastic model is employed. A change from static to dynamic compaction has no significant effect on subsequent behaviour.

KEYWORDS: compaction; earthfill; fabric/structure of soils; laboratory tests; partial saturation; suction.

Nous avons étudié l'influence de la pression de compaction, de la teneur en eau de compaction et du type de compaction (statique ou dynamique) sur le comportement subséquent du sol en faisant des essais triaxiaux à succion contrôlée sur des échantillons de kaolin speswhite compacté et non saturé. La pression compactante influence l'état initial, en déterminant la position initiale de la surface d'écoulement, affectant de la sorte et entre autres, la forme des courbes contrainte-déformation pendant le cisaillement. La pression de compaction influence aussi, dans un degré moindre, les positions des lignes de compression normales pour différentes valeurs de succion, mais elle n'a aucun effet sur les relations d'état critique. L'effet de la pression de compaction peut probablement être mis en maquette, purement en termes d'état initial si l'on emploie un modèle élasto-plastique anisotrope incorporant un durcissement rotationnel, alors que les paramètres définissant les pentes et les interceptions des lignes de compression normales pour diverses valeurs de succion, demandent à être ajustés en fonction de la variation de la pression de compaction si l'on emploie un modèle élasto-plastique isotrope conventionnel pour le durcissement. Le contenu en eau de compaction influence la succion initiale mais a également une influence substantielle sur les lignes de compression normales ainsi qu'un effet notable sur le comportement volumétrique aux états critiques. Il est probable que les échantillons de sol compactés avec différentes teneurs en eau devront être mis en maquette en tant que matériaux différents, qu'on emploie un modèle de durcissement élasto-plastique isotrope ou anisotrope pour le durcissement. Le passage d'une compaction statique à une compaction dynamique n'a aucun effet significatif sur le comportement ultérieur.

INTRODUCTION

The objective of the research presented in this paper and in the preceding companion paper (Sivakumar & Wheeler, 2000) was to investigate the influence of compaction procedure on the subsequent mechanical behaviour of an unsaturated compacted clay. This was done within the context of an elastoplastic critical state framework for unsaturated soil, to see which effects of a change in compaction procedure could be explained and modelled simply by variation in the initial compaction-induced state of the soil and which effects could be represented only by considering soils produced by different compaction procedures as fundamentally different materials.

Controlled-suction triaxial tests were performed on samples of unsaturated compacted speswhite kaolin, to examine the influences of compaction pressure, compaction water content and method of compaction (static or dynamic). Behaviour under isotropic stress states, including wetting under constant load and isotropic loading under constant suction, was explored in the companion paper. It was found that compaction pressure influenced the initial soil state (by controlling the initial location of the LC yield curve), but also influenced, to a limited degree,

the positions of the normal compression lines for different values of suction. Compaction water content influenced the initial soil state (by controlling the initial value of suction), but also had a significant influence on the positions of the normal compression lines. Finally, a change from static to dynamic compaction had no significant influence on the behaviour of this soil under isotropic stress states. In this second paper the work is extended to cover behaviour during shearing and implications for constitutive modelling.

Elastoplastic critical state framework

The soil behaviour is interpreted within the context of an elastoplastic critical state framework for unsaturated soil, initially developed by Alonso *et al.* (1987, 1990), with subsequent modifications suggested by Wheeler & Sivakumar (1995). The elastoplastic framework is expressed in terms of mean net stress \bar{p} , deviator stress q and matrix suction s , as defined in the companion paper (Sivakumar & Wheeler, 2000). Specific water volume v_w (the volume of water and solids in a volume of soil containing unit volume of solids) is used, in addition to specific volume v , to define fully the volumetric state of an unsaturated soil.

The form of the constitutive modelling framework for isotropic stress states was described in the companion paper. Extension to triaxial stress states involves development of the LC yield curve to form a yield surface in $q : \bar{p} : s$ space (see Alonso *et al.*, 1990). Inside this yield surface the soil behaviour

Manuscript received 2 November 1998; revised manuscript accepted 20 January 2000.

Discussion on this paper closes 26 November 2000; for further details see p. ii.

* University of Glasgow.

† Queen's University of Belfast.

is modelled as elastic, with compressive elastic volumetric strains produced by an increase of \bar{p} or an increase of s and elastic shear strains related to the change of q by an elastic shear modulus G . Plastic volumetric and shear strains commence once the yield surface is reached, with plastic volumetric strain increments given by an isotropic hardening law (Alonso *et al.*, 1990) and plastic shear strain increments by a suitable flow rule.

Under continuous shearing the model predicts that unsaturated soil will ultimately attain a critical state, with a unique critical state line in $q: \bar{p}: v$ space for each value of suction. Wheeler & Sivakumar (1995) suggested that the critical state lines could be represented by

$$q = M(s)\bar{p} + \mu(s) \quad (1)$$

$$v = \Gamma(s) - \psi(s)\ln\left(\frac{\bar{p}}{P_{at}}\right) \quad (2)$$

where $M(s)$, $\mu(s)$, $\Gamma(s)$ and $\psi(s)$ are functions of suction. Wheeler & Sivakumar (1995) assumed an elliptical shape for constant suction cross-sections of the yield surface joining normal compression states to critical states, and showed that this resulted in predicted test paths in $q: \bar{p}: v$ space that showed good agreement with experimental results from various types of controlled-suction triaxial shear tests on samples of compacted kaolin. The development of shear strain was also predicted with reasonable success by assuming an associated flow rule.

EXPERIMENTAL TESTS

Four series of controlled-suction triaxial tests, involving four different compaction procedures, were performed on samples of unsaturated compacted speswhite kaolin. Series 1 (originally reported by Wheeler & Sivakumar, 1995) involved samples statically compacted to a pressure of 400 kPa at a water content of 25% (4% dry of the optimum from standard Proctor compaction). In series 2 the compaction water content was unchanged, but the static compaction pressure was increased to 800 kPa (leading to a higher value of dry density). In series 3 the compaction water content was still 25%, but the method of compaction was altered from static to dynamic (with the compactive effort chosen so as to give the same dry density as in series 1). Finally, in series 4 the compaction water content was increased from 25 to 28.5%, with a static compaction pressure of 500 kPa selected so as to give approximately the same dry density as in series 2. Full details of the various compaction procedures are provided in the companion paper, together with details of the experimental equipment used for controlled-suction triaxial testing.

Each triaxial test consisted of three stages: an initial wetting stage at constant mean net stress \bar{p} (with the sample brought to a final suction of 300 kPa, 100 kPa or zero); an isotropic consolidation stage (performed at a constant suction of 300 kPa, 100 kPa or zero); and a final shearing stage. Procedures and results for the wetting and isotropic consolidation stages are provided in the companion paper.

Shearing stage

After the isotropic consolidation stage, each sample was sheared to failure at constant suction (of zero, 100 kPa or 300 kPa). Shearing was conducted at a constant displacement rate that gave a time to failure of approximately 15 days. Four different types of constant suction shearing were employed, by controlling pore air pressure u_a and pore water pressure u_w in different ways. Cell pressure σ_3 was held constant, rather than being used as a control variable during shearing, because it was inadvisable to reduce σ_3 during a test in the double-walled triaxial cell, as this could have caused exsolution of air bubbles within the cell fluid, which would have invalidated the measurement of sample volume change.

The four different types of shearing were as follows:

- (A) *Constant v /constant s shearing.* The control system was used to increase u_a and u_w by equal amounts (maintaining constant suction) as required to keep the sample volume constant.
- (B) *Constant \bar{p} /constant s shearing.* The control system was used to increase both u_a and u_w at one-third of the rate at which the deviator stress q was increasing (thus maintaining \bar{p} constant).
- (C) *Conventional constant s shearing.* Both u_a and u_w were held constant, giving $\Delta q/\Delta \bar{p} = 3$.
- (F) *Stress path constant s shearing.* The control system was used to vary u_a and u_w by equal amounts so as to follow a specified constant suction stress path (often involving several changes of $\Delta q/\Delta \bar{p}$).

Two other types of shearing, involving variation of suction, were also included in series 1 (see test types D and E in Wheeler & Sivakumar (1995)), but these tests are not reported here.

TEST RESULTS FROM SHEARING STAGE

The results from the shearing stage of the tests within series 1 were discussed in detail by Wheeler & Sivakumar (1995), and the intention here is to concentrate on comparisons between the different test series.

Stress-strain behaviour

Figure 1 shows plots of deviator stress q against axial strain ε_1 for twelve conventional constant suction shear tests (type C) all with $\Delta q/\Delta \bar{p} = 3$ and starting at $\bar{p} = 150$ kPa. At each value of suction the ultimate failure value of deviator stress is almost identical for the four test series, but the shapes of the stress-strain curves sometimes show marked differences.

The different shapes of stress-strain curves during shearing can be explained by considering the influence of compaction procedure on the initial location of the yield surface. Fig. 2 shows the approximate initial positions of the LC yield curve in the $s: \bar{p}$ plane produced by the four different compaction procedures, estimated from the results of the wetting and isotropic consolidation stages (see companion paper). Compaction to a higher value of dry density in series 2 and series 4 corresponded to significantly greater expansion of the LC yield curve (see LC₂ and LC₄ in Fig. 2) than occurred in series 1 or series 3 (see LC₁ and LC₃).

In Fig. 1(a) the stress-strain curves during shearing at zero suction are reasonably similar for all four methods of compaction, showing a normally consolidated form of response with no suggestion of a yield point. This is consistent with expectations; inspection of Fig. 2 shows that the preceding isotropic consolidation to $\bar{p} = 150$ kPa at zero suction (point A) would have resulted in substantial expansion of the yield curve in all four test series, so that the stress state at the start of shearing was on the yield surface in all cases (leading to plastic strains from the onset of shearing, and a normally consolidated form of response).

At a suction of 100 kPa (see Fig. 1(b)) the stress-strain curves for series 1 and series 3 show a normally consolidated form of response, whereas the curves for series 2 and series 4 show an initially stiff response, prior to a yield point (an overconsolidated form of behaviour). This is consistent with stress point B in Fig. 2 lying inside the initial position of the LC yield curve produced by the compaction procedures of series 2 and series 4, so that the initial section of the stress path during shearing lies inside the yield surface. Similar behaviour is observed in the tests at a suction of 300 kPa (see Fig. 2(c)), although there is some indication of a small initial section of high stiffness response in the test from series 1, suggesting that stress point C in Fig. 2 may lie just inside the yield curve location produced by the form of compaction used in series 1.

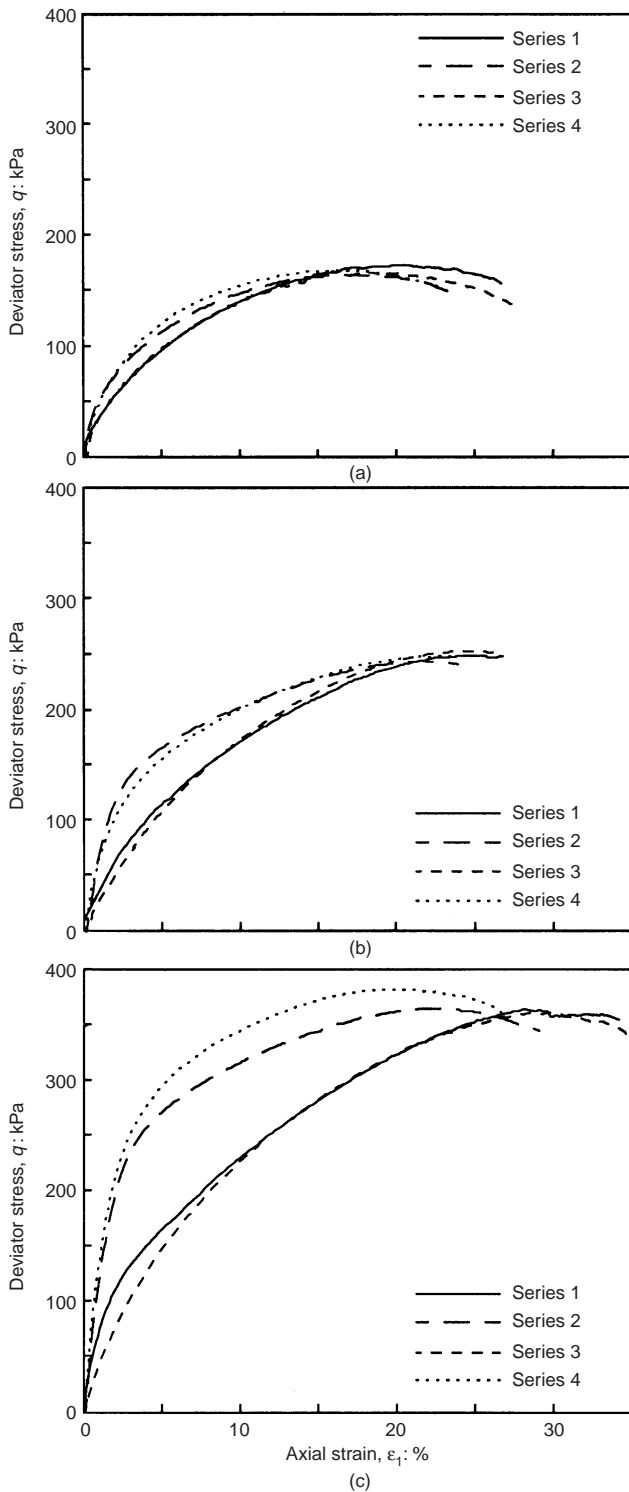


Fig. 1. Influence of compaction procedure on stress–strain curves during conventional constant suction shear tests with $\sigma_3 - u_a = 150$ kPa. (a) $s = 0$. (b) $s = 100$ kPa. (c) $s = 300$ kPa

Critical states

On termination of each test the state variables \bar{p} , q , s and v had approximately stabilized, suggesting attainment of a critical state. In some tests there was a very gradual post-peak reduction of deviator stress, but this was generally associated with the formation of a slip plane and was thought to represent a reduction towards a post-rupture value at very high local strain in the slip plane. Specific water volume v_w was still varying slightly at the end of all tests. This continuing variation of v_w could indicate simply that the tests were conducted too fast, resulting in incomplete equalization of pore water pressure (see

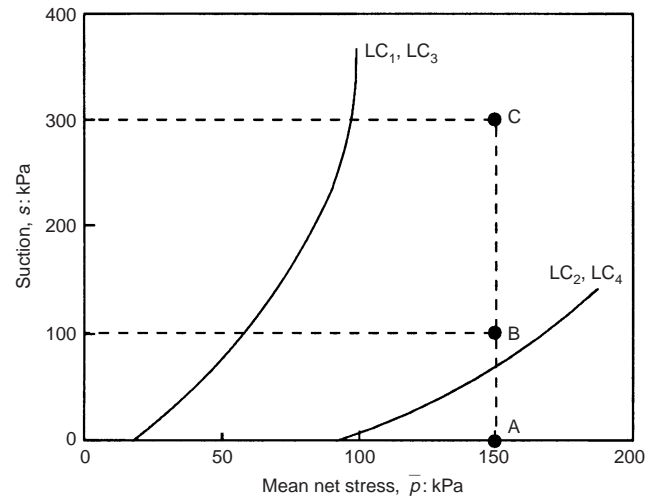


Fig. 2. Stress states at the start of shearing at $\sigma_3 - u_a = 150$ kPa, shown relative to approximate initial locations of yield curve

Wheeler & Sivakumar, 1995), or it could be due to slight dependence of v_w on shear strain (as suggested by Wheeler, 1996).

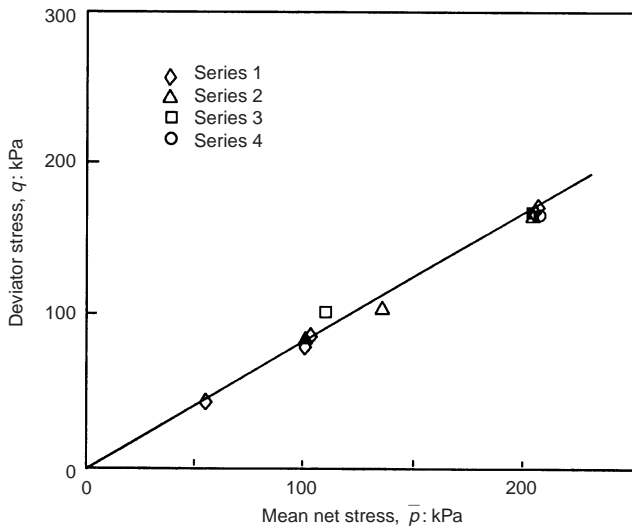
Figures 3–5 show the critical state values of q , v and v_w measured in all tests. Included in the figures are data from all four types of shear test (A, B, C and F). From Figs 3(a), 4(a) and 5(a) it is clear that, for each value of suction, the location of the critical state line in the $q : \bar{p}$ plane is the same for all four tests series. Inspection of Figs 3(b), 4(b) and 5(b) shows that for each value of suction the locations of the critical state line in the $v : \bar{p}$ plane (open data points) and $v_w : \bar{p}$ plane (solid data points) are the same for test series 1, 2 and 3, but that critical state values of v and v_w are typically slightly lower in series 4 than in the other test series. The best-fit lines shown in Figs 3(b), 4(b) and 5(b) are based on the experimental data points from series 1, 2 and 3 only.

Figure 6 shows the critical state lines identified from test series 1, 2 and 3 for the three different values of suction. In the $q : \bar{p}$ plot (Fig. 6(a)), the critical state lines at different values of suction are almost parallel, so that the critical state relationship of equation (1) simplifies to

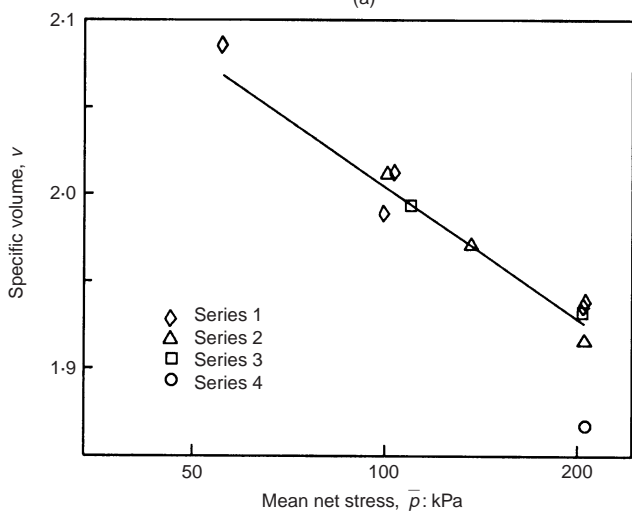
$$q = M\bar{p} + \mu(s) \quad (3)$$

with the suction-dependent parameter $M(s)$ replaced by a soil constant $M = 0.863$. In the $v : \bar{p}$ plane (Fig. 6(b)) the trend of the results is rather complex (as reported by Wheeler & Sivakumar, 1995). At low values of \bar{p} the critical state values of v at zero suction lie between those at suctions of 100 and 300 kPa, and the critical state lines for the three different values of suction tend to converge at high values of \bar{p} . In the $v_w : \bar{p}$ plane (Fig. 6(c)) the trends in the results are much clearer. As expected, critical state values of v_w decrease with increasing suction. In addition, the slope of the critical state line in the $v_w : \bar{p}$ plot decreases with increasing suction, with a negative slope observed at a suction of 300 kPa (this is predicted in the form of model proposed by Wheeler (1996)).

Initial conclusions on the influence of compaction procedure on behaviour during shearing can now be summarized. First, although increasing the compaction pressure may affect the shape of the stress–strain curve during shearing (as a result of the additional expansion of the yield surface during compaction), it has no apparent effect on the critical state relationships. This suggests that any differences in initial fabric caused by increased compaction pressure (observed in the influence on the normal compression lines, as reported in the companion paper) have been erased by shearing to a critical state. Secondly, a change from static to dynamic compaction has no significant effect on shear behaviour for speswhite kaolin compacted dry of optimum (consistent with the fact that there was no influence



(a)



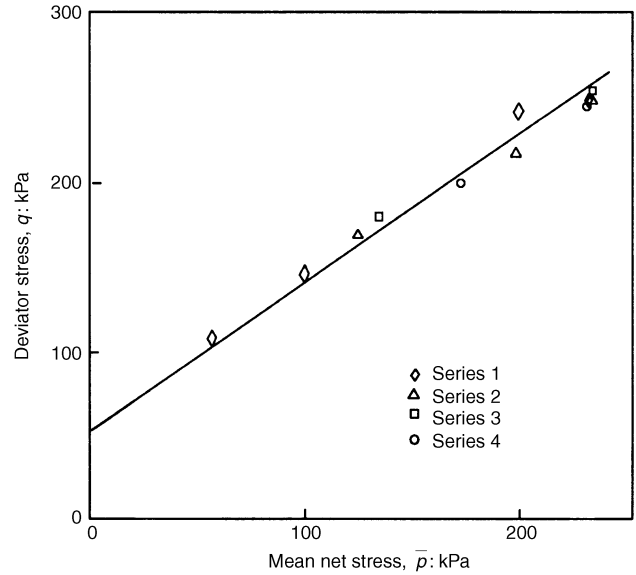
(b)

Fig. 3. Critical state data at $s = 0$

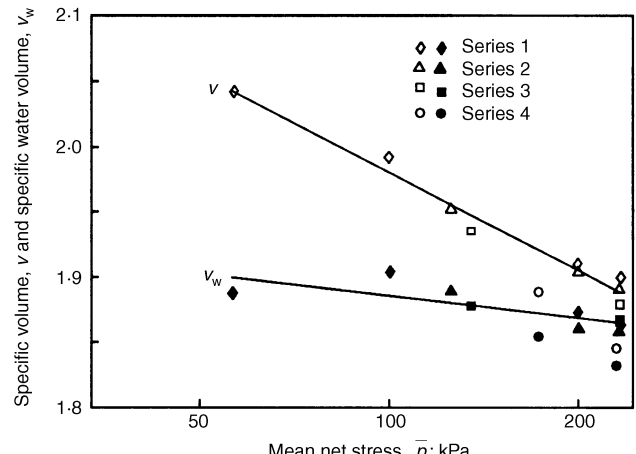
on behaviour under isotropic stress states). Finally, compaction at a higher water content has no effect on the locations of the critical state lines in the $q : \bar{p}$ plane, but does appear to affect slightly the critical state values of v and v_w . This suggests that differences in soil fabric produced by compaction at different water contents (strongly apparent in their influence on the normal compression lines, as described in the companion paper) are not completely erased even by shearing to a critical state. This is initially somewhat surprising, because a critical state is normally thought to represent a condition where fabric is being continuously destroyed. A possible explanation lies in the two levels of soil fabric within samples compacted dry of optimum: the macrostructural arrangement of large clay packets and interpacket voids, and the microstructure within individual packets. The critical states observed in triaxial tests probably correspond to shearing of the macrofabric to a critical state, whereas the relatively strong microfabric of individual clay packets may not reach a critical state, so that the influence of initial fabric is not completely erased.

IMPLICATIONS FOR CONSTITUTIVE MODELLING

If the existing elastoplastic constitutive models of Alonso *et al.* (1990) and Wheeler & Sivakumar (1995) are to be used, the experimental results presented here and in the companion paper suggest that the effects of changes in compaction pressure or compaction water content cannot be represented solely by



(a)



(b)

Fig. 4. Critical state data at $s = 100$ kPa

changes in the initial compaction-induced state of the soil (as represented by the initial location of the yield surface and the initial suction). In addition, the values of the parameters $N(s)$ and $\lambda(s)$, defining the normal compression lines for different values of suction, are dependent on both compaction pressure and compaction water content, and the parameters $\Gamma(s)$ and $\psi(s)$, defining the critical state lines in the $v : \bar{p}$ plane for different values of suction, seem to be dependent on compaction water content (but not compaction pressure). These additional effects are, presumably, due to the influence of compaction-induced soil fabric.

Influence of compaction pressure

The influence of an increase in compaction pressure on the fabric of samples compacted dry of Proctor optimum is probably limited to some compression of the large interpacket voids and stronger imprinting of the anisotropy of fabric induced by one-dimensional compaction. The compression of large interpacket voids during increased compaction is similar to that occurring during virgin loading after compaction (see Delage *et al.*, 1996), and this should therefore be represented simply by additional expansion of the yield surface in the existing elastoplastic models. A revised constitutive model, incorporating anisotropic hardening, would however be required in order to represent the stronger imprinting of fabric anisotropy. With such a constitutive model it may be possible to simulate all the

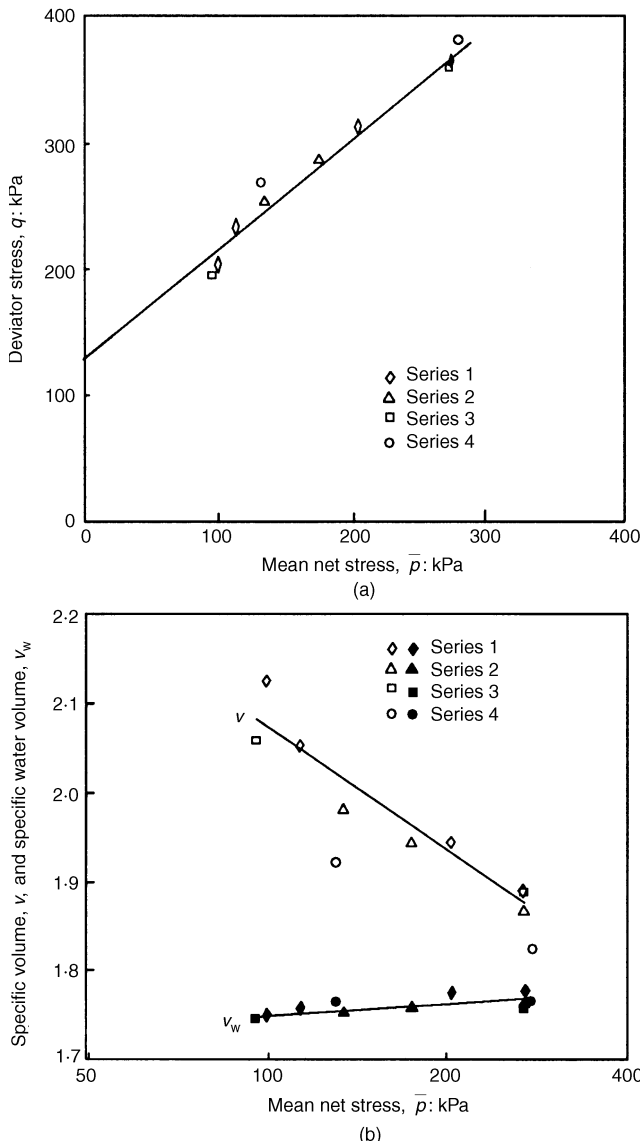


Fig. 5. Critical state data at $s = 300$ kPa

effects of changes in compaction pressure solely by variation in the initial state of the soil. In particular, the influence of anisotropy can be used to explain why the post-yield behaviour during isotropic loading at a given value of suction shows some dependence on compaction pressure.

Induced anisotropy can be represented by an elastoplastic model involving a rotational component of hardening, so that yield curves can be inclined in the $q : \bar{p}$ plane. Cui & Delage (1996) present experimental data from tests on an unsaturated compacted silt which show that after one-dimensional compaction constant suction yield curves are inclined in the $q : \bar{p}$ plane, with the major axis of each curve coinciding approximately with the K_0 line. Data from tests on a collapsible unsaturated silty soil performed by Maatouk *et al.* (1995) also suggest inclined yield curves. These results are, of course, entirely consistent with the inclined shapes of yield curve reported for many saturated natural clays with one-dimensional depositional histories (e.g. see Mitchell, 1970; Graham *et al.*, 1983). Zakaria *et al.* (1995) present results from tests on compacted unsaturated speswhite kaolin (prepared in an identical fashion to the tests in series 1 reported here), which show that subsequent isotropic compression to much higher stress states results in gradual erasure of the initial anisotropy induced by one-dimensional compaction, until the major axis of each constant suction yield curve is approximately aligned along the \bar{p} axis.

Figure 7 shows the form of behaviour during constant suction

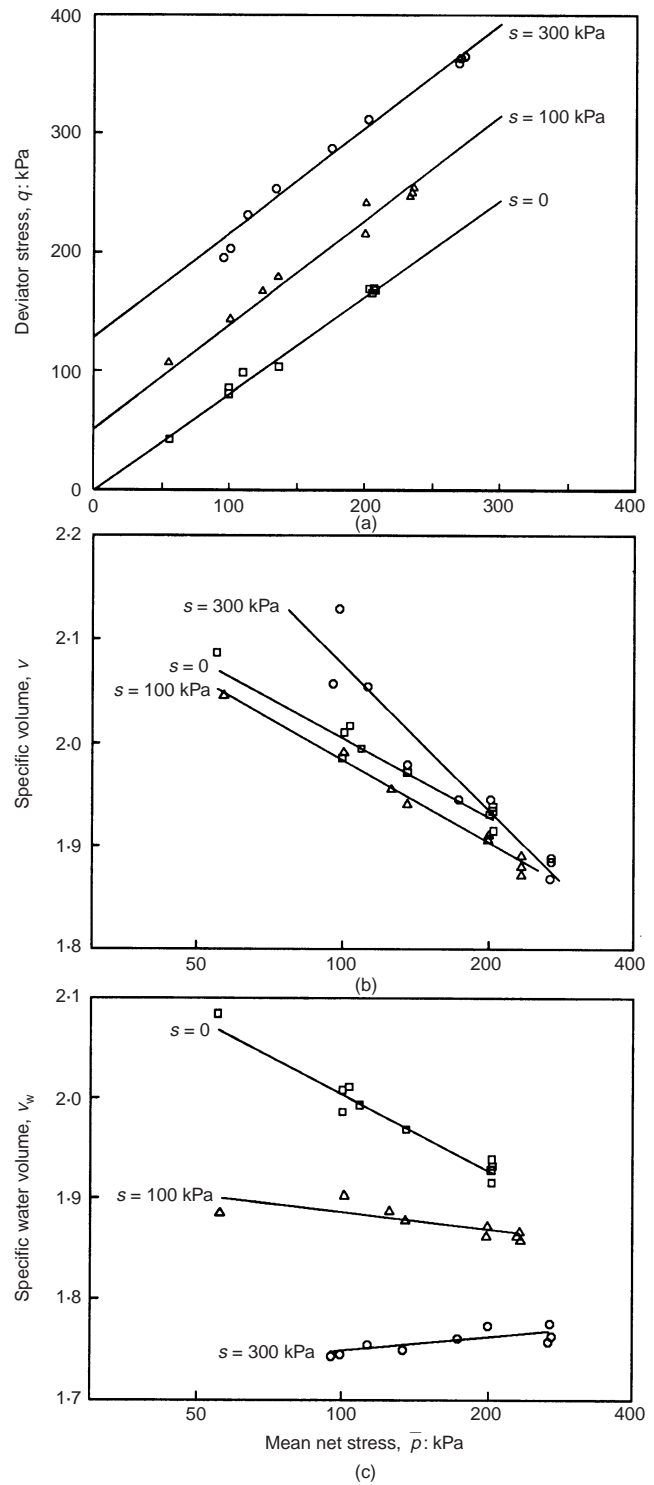


Fig. 6. Critical state data for series 1, 2, and 3

isotropic compression of a one-dimensionally compacted sample that would be predicted by an elastoplastic model involving rotational and isotropic components of hardening (e.g. see Wheeler, 1997). In models of this type the yield curve is typically in the form of a sheared or rotated ellipse, with the size and inclination of the yield curve defined by the values of the parameters \bar{p}_m and α , respectively (see Fig. 7(a)). A change in the size of the yield curve, as defined by the value of \bar{p}_m , is assumed to be related solely to the plastic volumetric strain ϵ_v^p . In addition, however, rotation of the yield curve (a change in the value of α) occurs with plastic straining if the current inclination of the curve differs from an equilibrium value corresponding to the current stress state. Any variation in the

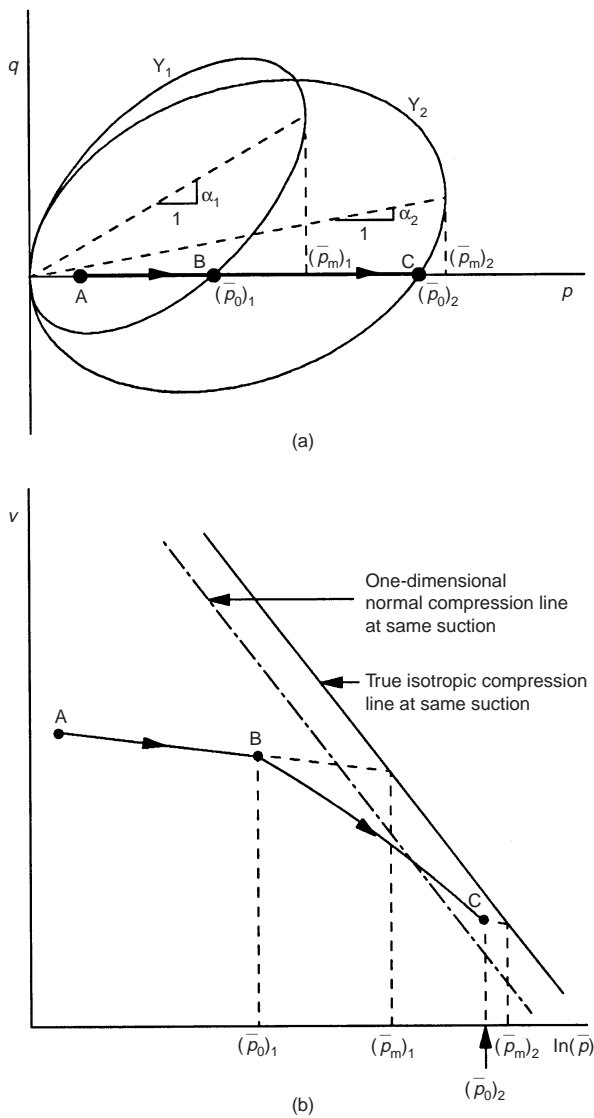


Fig. 7. Elastoplastic model incorporating rotational component of hardening

value of α represents a change in the degree of anisotropy of the soil.

In Fig. 7, a soil sample is isotropically compressed at constant suction along path ABC, with the yield curve for this value of suction initially in the inclined position Y_1 , due to the previous one-dimensional compaction. Yield occurs at B, at a mean net stress $(\bar{p}_0)_1$, but at this point the accumulated plastic volumetric strain is the same as for a sample with a purely isotropic stress history loaded at the same suction to a higher value of mean net stress $(\bar{p}_m)_1$ (see Fig. 7(a)). In the $v : \bar{p}$ plane, the value of specific volume at B therefore lies considerably below the true isotropic normal compression line for the same value of suction (see Fig. 7(b)), and even below the corresponding one-dimensional normal compression line. On loading from B to C the yield curve expands and rotates clockwise to a new position Y_2 . At point C, at a stress $(\bar{p}_0)_2$, the accumulated plastic volumetric strain is the same as for a sample with an isotropic history at stress $(\bar{p}_m)_2$. In the $v : \bar{p}$ plane point C still lies below the true isotropic normal compression line, but the gap has reduced, because of the influence of yield curve rotation. On subsequent compression to higher values of \bar{p} the observed compression curve gradually converges with the true isotropic normal compression line, as the inclination of the yield curve decreases. This is the same behaviour that would be observed in a saturated sample prepared under

one-dimensional consolidation and then compressed isotropically (see Wheeler, 1997).

Figure 8 shows the forms of behaviour that would be predicted, by the type of anisotropic hardening model described above, for two samples of the same soil one-dimensionally compacted to different pressures and then each isotropically loaded at the same value of suction. Not only does the sample compacted to the higher pressure yield at a higher mean net stress, but also the post-yield curve lies below the corresponding curve for the sample compacted to the lower pressure, because higher stresses are required to produce convergence with the true isotropic normal compression line for the given value of suction. Comparison of Fig. 8 with the experimental results for the isotropic consolidation stages of the tests in series 1 and series 2, presented in the companion paper, shows excellent qualitative agreement. The proposed form of anisotropic hardening elastoplastic model would therefore appear capable of modelling the observed influence of compaction pressure solely in terms of the initial soil state (as defined by initial suction and initial size and inclination of the yield surface).

The experimental data from the tests in series 1 and series 2 show no influence of compaction pressure on the critical state relationships. To successfully represent this aspect of behaviour, the form of rotational hardening within an anisotropic elastoplastic model has to be such that the final inclination of the yield curve on reaching a critical state is independent of the previous stress history, as, for example, in the models of Wheeler (1997) or Nääätänen *et al.* (1999).

Another feature of compacted soil behaviour that can be explained by an elastoplastic model incorporating a rotational component of hardening is the relatively low values of yield stress observed during isotropic compression after one-dimensional compaction. The tests in series 1 can be considered as an example. In these tests an axial net stress $\sigma_1 - u_a$ of 400 kPa was applied during compaction (compaction was sufficiently slow that it is reasonable to assume full dissipation of excess pore air pressure, given the existence of inter-connected air voids). Even allowing for a K_0 value of less than 1 during the application of compaction load, it is unlikely that the value of mean net stress \bar{p} during compaction was significantly less than 300 kPa. At first sight it therefore appears somewhat surprising that the initial position of the LC yield curve estimated from the subsequent isotropic compression behaviour involves such

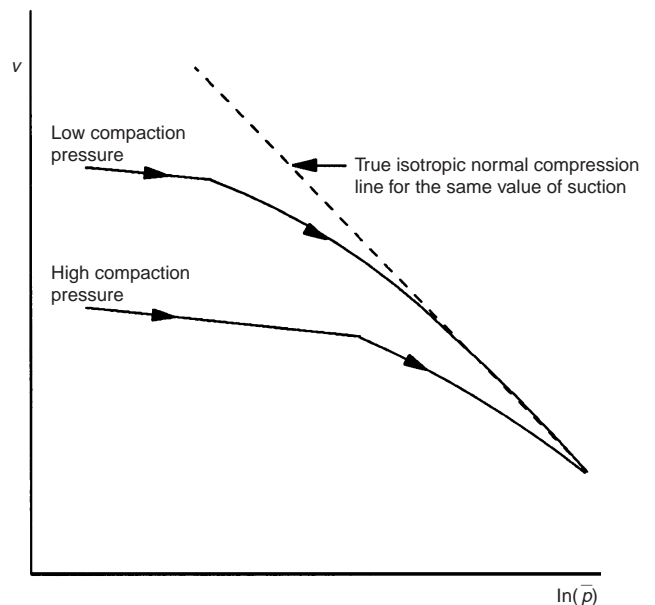


Fig. 8. Qualitative influence of compaction pressure on isotropic compression behaviour predicted by rotational hardening model

low values of yield stress (an isotropic yield stress of less than 200 kPa has been measured in an additional test performed at a suction of 700 kPa, corresponding approximately to the suction present at the end of compaction). This apparent discrepancy, between the value of \bar{p} applied during one-dimensional compaction and the much lower yield value of \bar{p} observed during subsequent isotropic compression, is, of course, explained if the yield curve is inclined in the $q: \bar{p}$ plane (see Fig. 7(a)). Similar behaviour was reported by Cui & Delage (1996) in their tests, and they suggested the same explanation.

Influence of compaction water content

Changes of compaction water content are likely to have a more radical influence on soil fabric than changes of compaction pressure. These effects of compaction water content could include a change from a double-structure fabric with a bimodal pore size distribution to a more uniform fabric with a uni-modal pore size distribution (Delage *et al.*, 1996). Therefore, whereas an anisotropic elastoplastic model with a rotational component of hardening would probably be capable of representing the influence of changes in compaction pressure solely in terms of initial soil state, it is unlikely that the influence of changes in compaction water content could be represented in any elastoplastic model simply in terms of initial soil state. Instead, it is likely that proper modelling of the influence of compaction water content will require that soils compacted at different water contents are treated as different materials. This suggestion is supported by the experimental results presented in this paper and in the companion paper, which show that soil parameters such as $N(s)$, $\lambda(s)$, $\Gamma(s)$ and $\psi(s)$ would be dependent on compaction water content.

CONCLUSIONS

The results of controlled-suction triaxial tests on samples of unsaturated compacted speswhite kaolin indicate that, as expected, compaction pressure strongly influences the initial state of a sample, mainly by controlling the initial location of the yield surface in $q: \bar{p}: s$ space. This can produce a significant effect on the form of the stress-strain curve during shearing, particularly the shear stiffness during the early stages of shearing. Although it was found in the companion paper that compaction pressure also affects slightly the positions of the normal compression lines for different values of suction, suggesting some influence on the initial compaction-induced soil fabric, critical state relationships were found to be independent of compaction pressure, indicating that fabric differences caused by a change of compaction pressure are of a type that can be erased by shearing to a critical state.

A change of compaction water content produces a more radical effect on subsequent soil behaviour (in addition to the expected influence on the initial soil state, through the value of suction produced by compaction). Not only are the positions of the normal compression lines for different values of suction significantly affected, but the locations of the critical state lines in the $v: \bar{p}$ plane and the $v_w: \bar{p}$ plane (but not the $q: \bar{p}$ plane) appear to be dependent on compaction water content. This suggests that differences of soil fabric caused by a change of compaction water content, such as a change from a double-structure fabric to a more uniform fabric, continue to influence soil behaviour even after shearing to a critical state.

For speswhite kaolin compacted dry of optimum, a change from static compaction to dynamic compaction (without change of compaction water content or compaction-induced dry density) has no apparent effect on subsequent soil behaviour.

The mechanical behaviour of unsaturated compacted clays can be represented by elastoplastic critical state constitutive models, with suction employed as an additional stress state variable. In applying a model of this type, the initial state of the soil is determined by the compaction procedure, with the initial suction controlled mainly by the compaction water content and the initial location of the yield surface controlled

mainly by the dry density (or void ratio) achieved during compaction. In addition, however, accurate modelling requires that the influence of changes in compaction-induced soil fabric are included. If the existing isotropic hardening elastoplastic models of Alonso *et al.* (1990) or Wheeler & Sivakumar (1995) are employed, this means that the soil parameters $N(s)$ and $\lambda(s)$ (defining the normal compression lines for different values of suction) must be adjusted with both compaction pressure and compaction water content, whereas the parameters $\Gamma(s)$ and $\psi(s)$ (defining the critical state lines) must be adjusted solely with compaction water content.

Changes of soil fabric produced by increasing the compaction pressure consist of compression of large inter-packet voids (consistent with increased expansion of the yield surface) and a stronger imprinting of compaction-induced fabric anisotropy. The effect of both of these effects could be modelled solely in terms of the initial state of the soil by employing an elastoplastic model with a rotational component of hardening. It appears unlikely that the effects of variation in compaction water content can be modelled in a similar fashion, because changes of soil fabric produced by variation in the compaction water content are of a more radical nature. Two batches of the same soil compacted at different water-contents may therefore have to be treated as fundamentally different materials.

ACKNOWLEDGEMENTS

The triaxial tests were performed at the University of Sheffield and the University of Oxford, with financial support from the UK Engineering and Physical Sciences Research Council.

NOTATION

G	shear modulus
\bar{p}	mean net stress $((\sigma_1 + 2\sigma_3)/3 - u_a)$
p_{at}	atmospheric pressure
\bar{p}_m	maximum value of \bar{p} on yield curve
\bar{p}_0	yield value of \bar{p} under isotropic stress state
q	deviator stress $(\sigma_1 - \sigma_3)$
s	matrix suction $(u_a - u_w)$
u_a	pore air pressure
u_w	pore water pressure
v	specific volume $(1 + e)$
v_w	specific water volume $(1 + S_r e)$
$\lambda(s), N(s)$	slope and intercept of normal compression line in $v: \ln(\bar{p}/p_{at})$ plot
$M(s), \mu(s)$	slope and intercept of critical state line in $q: \bar{p}$ plot
σ_1, σ_3	axial and radial total stresses
$\psi(s), \Gamma(s)$	slope and intercept of critical state line in $v: \ln(\bar{p}/p_{at})$ plot

REFERENCES

- Alonso, E. E., Gens, A. & Hight, D. W. (1987). Special problem soils. General report. *Proc. 9th Eur. Conf. Soil. Mech. Found. Eng., Dublin* **3**, 1087–1146.
- Alonso, E. E., Gens, A. & Josa, A. (1990). A constitutive model for partially saturated soils. *Géotechnique* **40**, No. 3, 405–430.
- Cui, Y. J. & Delage, P. (1996). Yielding and plastic behaviour of an unsaturated compacted silt. *Géotechnique* **46**, No. 2, 291–311.
- Delage, P., Audiguier, M., Cui, Y.-J. & Howat, M. D. (1996). Microstructure of a compacted silt. *Can. Geotech. J.* **33**, 150–158.
- Graham, J., Noonan, M. L. & Lew, K. V. (1983). Yield states and stress-strain relationships in a natural plastic clay. *Can. Geotech. J.* **20**, 502–516.
- Maatouk, A., Leroueil, S. & La Rochelle, P. (1995). Yielding and critical state of a collapsible unsaturated silty soil. *Géotechnique* **45**, No. 3, 465–477.
- Mitchell, R. J. (1970). On the yielding and mechanical strength of Leda clays. *Can. Geotech. J.* **7**, 297–312.
- Näätänen, A., Wheeler, S., Karstunen, M. & Lojander, M. (1999). Experimental investigation of an anisotropic hardening model for soft clays. *Proc. 2nd Int. Symp. Pre-failure Deform. Character. of Geomaterials, Torino* **1**, 541–548.
- Sivakumar, V. & Wheeler, S. J. (2000). Influence of compaction procedure on the mechanical behaviour of an unsaturated compacted clay. Part 1: wetting and isotropic compression.

- Wheeler, S. J. (1996). Inclusion of specific water volume within an elasto-plastic model for unsaturated soil. *Can. Geotech. J.* **33**, 42–57.
- Wheeler, S. J. (1997). A rotational hardening elasto-plastic model for clays. *Proc. 14th Int. Conf. Soil. Mech. Found. Eng., Hamburg* **1**, 431–434.
- Wheeler, S. J. & Sivakumar, V. (1995). An elasto-plastic critical state framework for unsaturated soil. *Géotechnique* **45**, No. 1, 35–53.
- Zakaria, I., Wheeler, S. J. & Anderson, W. F. (1995). Yielding of unsaturated compacted kaolin. *Proc. 1st Int. Conf. Unsaturated Soils, Paris* **1**, 223–228.